Polarization transfer in the $^{16}O(p,p')$ reaction at forward angles and structure of the spin-dipole resonances

T. Kawabata,* T. Ishikawa, M. Itoh, M. Nakamura, H. Sakaguchi, H. Takeda, T. Taki,† M. Uchida, Y. Yasuda, and M. Yosoi
Department of Physics, Kyoto University, Kyoto 606-8502, Japan

H. Akimune and K. Yamasaki
Department of Physics, Konan University, Kobe, Hyogo 658-8501, Japan

G. P. A. Berg, H. Fujimura, K. Hara, K. Hatanaka, J. Kamiya, T. Noro,‡ E. Obayashi, T. Wakasa, and H. P. Yoshida
Research Center for Nuclear Physics, Osaka University, Ibaraki, Osaka 567-0047, Japan

B. A. Brown
Department of Physics and Astronomy and National Superconducting Laboratory, Michigan State University, East Lansing, Michigan 48824-1321

H. Fujita, Y. Fujita, Y. Shimbara, and H. Ueno§
Department of Physics, Osaka University, Toyonaka, Osaka 560-0043, Japan

M. Fujiwara
Research Center for Nuclear Physics, Osaka University, Ibaraki, Osaka 567-0047, Japan and Advanced Science Research Center, Japan Atomic Energy Research Institute, Tokai, Ibaraki 319-1195, Japan

K. Hosono
Department of Engineering, Himeji Institute of Technology, Hyogo 678-1297, Japan

A. Tamii
Department of Physics, University of Tokyo, Hongo, Tokyo 113-0033, Japan

H. Toyokawa
Japan Synchrotron Radiation Research Institute, Hyogo 679-5198, Japan
(Received 8 January 2002; published 6 June 2002)

Cross sections and polarization transfer observables in the $^{16}O(p,p')$ reactions at 392 MeV were measured at several angles between $\theta_{lab}=0°$ and 14°. The non-spin-flip ($\Delta S=0$) and spin-flip ($\Delta S=1$) strengths in transitions to several discrete states and broad resonances in ^{16}O were extracted using a model-independent method. The giant resonances in the energy region of $E_x=19-27$ MeV were found to be predominantly excited by $\Delta L=1$ transitions. The strength distribution of spin-dipole transitions with $\Delta S=1$ and $\Delta L=1$ were deduced. The obtained distribution was compared with a recent shell model calculation. Experimental results are reasonably explained by distorted-wave impulse-approximation calculations with the shell model wave functions.

DOI: 10.1103/PhysRevC.65.064316 PACS number(s): 24.30.Cz, 24.70.+s, 25.40.Ep, 27.20.+n

I. INTRODUCTION

Spin-isospin excitation modes in nuclei have been studied intensively, not only because they are of interest in nuclear structure, but also because the relevant operators mediate β-decay and neutrino capture processes. The cross sections of hadronic reactions provide a good measure for the weak interaction response, which is a key ingredient in studies of nucleosynthesis. Gamow-Teller resonances ($\Delta T=1$, $\Delta S=1$, $\Delta L=0$) mediated by the $\vec{\sigma}\vec{\tau}$ operator have been systematically investigated by charge exchange reactions like (p,n) and $(^3\mathrm{He},t)$ reactions with a selectivity for spin-flip transitions at intermediate energies [1,2]. On the other hand, spin-dipole resonances (SDR; $\Delta T=1$, $\Delta S=1$, $\Delta L=1$) mediated by the $\vec{\sigma}\vec{\tau}rY_1$ operator have not been studied in any detail although the excitations have recently received attention from the viewpoint of detection of supernova neutrinos [3–5]. The detailed structure of the SDR remains unclear

*Present address: Research Center for Nuclear Physics, Osaka University, Ibaraki, Osaka 567-0047, Japan. Email address: takahiro@rcnp.osaka-u.ac.jp

†Present address: Asaka Technology Development Center, Fuji Photo Film Co., Ltd., Asaka, Saitama 351-8585, Japan.

‡Present address: Department of Physics, Kyushu University, Fukuoka 812-8581, Japan.

§Present address: RIKEN (The Institute for Physical and Chemical Research), Wako, Saitama 351-0198, Japan.

with respect to the three different spin states of $J^\pi=2^-$, 1^-, and 0^-.

Transitions to the 1^- states can be induced by a probe with spin through the spin-flip and non-spin-flip processes with the $\vec{\sigma}\vec{\tau}rY_1$ and $\vec{\tau}rY_1$ operators. The $\vec{\tau}rY_1$ operator mediates the isovector giant dipole resonance (IVGDR; $\Delta T=1$, $\Delta S=0$, $\Delta L=1$), which has the spin parity of $J^\pi=1^-$, the same as the SDR. Theoretically, the SDR and IVGDR are observed together in (p,p') reactions because they have the same $J^\pi=1^-$ and are located in the same excitation energy region. In fact, it is experimentally confirmed in the polarization transfer measurements [6]. The problem concerning the coexistence of the SDR and IVGDR was discussed in Ref. [7].

The SDR in the $A=12$ system has been relatively well studied in the past. Cross sections of the SDR in the $^{12}C(p,n)$ reaction were measured at various bombarding energies and the strength distributions were discussed and compared with shell model calculations in view of the analog relation in $N=Z$ nuclei [8]. The experimental analysis of the data has led to the conclusion that broad structures at $E_x=4.2$ and 7.2 MeV in ^{12}N consist of mainly 2^- and 1^-, respectively. This conclusion is consistent with the results obtained from the vertical polarization-transfer measurements in the $^{12}C(p,p')$ reaction at $E_p=318$ MeV [9]. Recent measurements of (p,n) and (n,p) reactions supported this conclusion [10]. An analysis of the tensor analyzing powers measured in the $^{12}C(d,^2He)$ reaction resulted in the contradictory conclusion that the 2^- transition dominates around $E_x=7.5$ MeV in ^{12}B, which corresponds to the excitation region around $E_x=7.2$ MeV in ^{12}N, and the contribution from the 1^- transition is small [11]. This "*missing spin-flip* 1^-" result was supported by a shell model study, which predicted that the tensor correlation and the mixing of $2p$-$2h$ configurations push the spin-flip 1^- strength to higher excitation energies and thus quench the strength around the giant resonance region [12]. However, more recent measurements of neutron decay in the SDR region excited via the $(d,^2He)$ reaction supported the (p,n) and (n,p) results again [13]. Thus, this problem concerning the spin-parity assignment for the SDR in the $A=12$ system remains controversial.

The ^{16}O nucleus consists of eight protons and eight neutrons in the $1s_{1/2}$, $1p_{3/2}$, and $1p_{1/2}$ shell orbitals in a simple independent particle model. Since the SDR excitation in p-shell nuclei is described as a coherent sum of $1p$-$1h$ transitions from the p- to the sd-shell orbitals, the SDR excitations in ^{16}O are expected to be stronger than those in ^{12}C. Djalali *et al.* identified several 2^- and 1^- states at $E_x=19-27$ MeV in ^{16}O by comparing a (p,p') spectrum at $E_p=201$ MeV with a (γ,n) spectrum [14]. They pointed out that the gross structures of the 1^- resonances observed in (p,p') and (γ,n) reactions are similar. This suggests that the IVGDR, which is excited through the Coulomb interaction, is dominant in the proton inelastic scattering at intermediate energies, especially at forward angles. Therefore, spin-flip 1^- states were not identified in the (p,p') measurement of Ref. [14].

It is well known that the analog states of $N=Z$ nuclei can be easily observed in charge exchange reactions. Fazely *et al.* identified two strong 2^- states at $E_x=0.4$ and 7.6 MeV and two broad 1^- states at 9.4 and 11.5 MeV in ^{16}F by measuring angular distributions of the $^{16}O(p,n)$ cross sections [15]. In addition, Hicks *et al.* [16] and Mercer *et al.* [17] reported that a sizable amount of the $\Delta L=1$ strength in ^{16}F and ^{16}N was observed in the $^{16}O(p,n)$ and $^{16}O(n,p)$ reactions using a multipole decomposition method. In their multipole decomposition analyses, spin-flip and non-spin-flip contributions of the $\Delta L=1$ strength were not distinguished. Since the (p,n) and (n,p) reactions at intermediate energies dominantly carry the spin-flip strength at forward angles, the $\Delta L=1$ strength in the $^{16}O(p,n)$ and $^{16}O(n,p)$ reactions should include the $\Delta S=1$ (SDR) components. Watson *et al.* performed a high-resolution measurement of the $^{16}O(p,n)$ reaction at $E_p=135$ MeV and identified 2^-, 1^-, and 1^+ transition strengths by measuring cross sections and vertical polarization transfer (PT) observables [18]. For further clarification of the spin nature of the 1^- transitions, it is, however, necessary to measure horizontal PT observables, too.

There is another important aspect in studying the level structure of the excited states in ^{16}O. The nucleus ^{16}O is now considered as a possible neutrino detector to investigate the explosion mechanism of supernovae [5,19–23]. High energy neutrinos with an average energy of ≈ 25 MeV are emitted from the heat bath in a supernova. When a supernova collapses near our galaxy, it is expected that a sizable flux of neutrinos from the neutronization process and the subsequent thermal emission process appears on the earth during a subsecond period. Such supernova neutrinos can be detected by measuring deexcitations of the excited states in ^{16}O, ^{16}F, and ^{16}N in large neutrino detectors, e.g., Superkamiokande and SNO with a huge number of ^{16}O nuclei. The neutrinos predominantly excite 0^-, 1^-, and 2^- states via neutral and charged current reactions [5]. Many calculations were performed to estimate the cross sections of neutrino induced reactions on ^{16}O [19,21–23]. To confirm these calculations, measurements of the strength distributions of 0^-, 1^-, and 2^- states in ^{16}O are important not only for nuclear physics but also for the astrophysical application.

Recently, all the PT observables for (p,p') reactions were successfully measured at $0°$ and were found to be a useful spectroscopic tool to study nuclear structure [24,25], because the total spin transfer $\Sigma\equiv[3-(D_{SS}+D_{NN}+D_{LL})]/4$ provides a clear means to clarify spin-flip or non-spin-flip transitions [26,27]. Thus, measurements of PT observables at forward angles enable us to extract spin-flip transitions. In this report, we will present information on the structure of the SDR in ^{16}O, which is obtained from measurements of PT observables in proton inelastic scattering at very forward angles including $0°$.

II. EXPERIMENTAL PROCEDURE

The experiment was performed at the Research Center for Nuclear Physics (RCNP), Osaka University by using a 392-MeV polarized proton beam accelerated by the coupled cyclotrons. The proton beam from the polarized ion source [28]

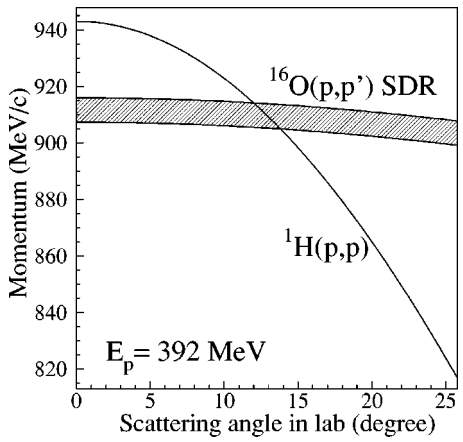

FIG. 1. Momentum of protons scattered from ^{1}H and ^{16}O at $E_p=392$ MeV as a function of angles. The hatched region shows the momentum region of protons exciting the SDR (19 MeV $\leqslant E_x \leqslant 25$ MeV).

was accelerated to a kinetic energy of 64.2 MeV by the $K=120$ MeV AVF (azimuthally varying field) cyclotron, and was further boosted to 392 MeV by the $K=400$ MeV ring cyclotron. The proton beam extracted from the ring cyclotron was achromatically transported to the target. The beam intensity on target was in the range of 1–10 nA. Scattered protons were momentum analyzed by the high-resolution spectrometer Grand Raiden [29]. Trajectories of the scattered protons were determined using a focal-plane detector system consisting of two multiwire drift chambers and plastic scintillation detectors. Cross sections were obtained at seven scattering angles between $\theta_{lab}=0°$ and 14°. An energy resolution of 80–150 keV full width at half maximum, was obtained, which was dominated by the energy spread of the cyclotron beam. In the measurements at scattering angles between 6° and 14°, the proton beam was stopped in a Faraday cup in the scattering chamber. Since this Faraday cup reduced the acceptance of the spectrometer Grand Raiden at angles between 2.5° and 4° and an unacceptable background from edge scattering was produced, a different Faraday cup was used between the first quadrupole and the sextupole magnets of Grand Raiden [29] at these angles. In the measurement at 0°, the proton beam passed through Grand Raiden and was stopped in another Faraday cup located 12 m downstream of the focal plane [30].

A. H_2O target

Thin H_2O ice sheets with various thicknesses of 10–30 mg/cm^2 were used as oxygen targets. The ice target system is described in detail in Ref. [31]. Here, we briefly describe the target preparation procedure. Self-supporting ice sheets made of pure water were mounted in the scattering chamber, which was kept under vacuum lower than 10^{-3} Pa without any window foil. The ice targets were cooled down to below 140 K by liquid nitrogen. The loss of the ice target by sublimation is negligible at this temperature, since vapor pressure of H_2O is of the order of 10^{-6} Pa at 140 K and decreases exponentially at lower temperature. This newly developed ice target gave us the great advantage in obtaining clean (p,p') spectra since the background events from hydrogen contaminations in the target are out of the interested momentum region at most of the measurement angles due to the large difference of kinematic effects between oxygen and hydrogen. Figure 1 shows the kinematics of protons scattered from ^{1}H and ^{16}O as a function of angles. In measurements for the SDR region ($E_x=19$–25 MeV) denoted by the hatched region in Fig. 1, the $^{16}O(p,p')$ events are obscured by the $^{1}H(p,p)$ events at $\theta_{lab}=12°-14°$, but are not disturbed at the other angles.

In order to monitor the target thickness during the measurement, elastic scattering events from hydrogen were measured by the spectrometer LAS [32] placed at $\theta_{lab}=59.5°$. The target thickness was calibrated by using the cross section for proton-proton elastic scattering at $\theta_{lab}=59.5°$ calculated with the program SAID [33]. The target thickness was stable within the measurement uncertainty of $\pm 2.5\%$ during the experiment.

B. Polarization transfer measurements

A proton beam from the AVF cyclotron was vertically polarized. Two superconducting solenoids between the two cyclotrons were used for the purpose of rotating the polarization axis of protons from the vertical to the horizontal direction in measurements with a horizontally polarized beam. The two solenoids were located upstream and downstream of bending magnets with a total bending angle of 45°. This configuration enables us to obtain horizontally polarized beams with two polarization axes approximately perpendicular to each other. The beam polarization was 0.6–0.8, which was monitored with an accuracy of ± 0.02 by two sets of beam-line polarimeters after the ring cyclotron using a polystyrene analyzer target. The direction of the beam polarization was reversed every second to eliminate instrumental asymmetries.

The polarization of protons scattered from the ice target were measured at laboratory angles of 0°, 4°, and 8° by a focal plane polarimeter (FPP) after momentum analysis in the spectrometer Grand Raiden. The FPP consisted of an analyzer target of a 12-cm-thick carbon slab, four multiwire proportional chambers, and scintillator hodoscopes [34]. The effective analyzing power A_y^{eff} of the FPP is given by

$$A_y^{eff}=\frac{\int \sigma^{inc}(\theta)A_y^{inc}(\theta)\cos\phi\, d\Omega}{\int \sigma^{inc}(\theta)\, d\Omega}, \qquad (1)$$

where $\sigma^{inc}(\theta)$ and $A_y^{inc}(\theta)$ are the cross section and analyzing power for inclusive proton scattering from elastic, inelastic, and quasifree processes in the analyzer target of the FPP. The angular integrations in Eq. (1) are performed over the polar angle of $5°\leqslant\theta\leqslant 20°$ and the azimuthal angle of $|\phi| \leqslant 66.8°$ for the scattering angles. The inclusive cross section $\sigma^{inc}(\theta)$ was measured in this experiment. We used the ana-

lyzing power $A_y^{inc}(\theta)$ given in Ref. [35], which is parametrized as a function of the proton energy and scattering angle.

The PT observables ($D_{I'J}$) are defined by the following relation [36,37]:

$$\begin{pmatrix} p'_{S'} \\ p'_{N'} \\ p'_{L'} \end{pmatrix} = \frac{1}{1+p_N A_N} \left[\begin{pmatrix} 0 \\ P \\ 0 \end{pmatrix} + \begin{pmatrix} D_{S'S} & 0 & D_{S'L} \\ 0 & D_{N'N} & 0 \\ D_{L'S} & 0 & D_{L'L} \end{pmatrix} \times \begin{pmatrix} p_S \\ p_N \\ p_L \end{pmatrix} \right]. \quad (2)$$

The symbols p_I and $p'_{I'}$ ($I=S, N, L$), denote the polarizations of the incident and the scattered protons, respectively. The coordinate system is chosen so that the L axis is along the beam direction, the N axis is along the normal to the horizontal plane, and the S axis is chosen to form a right-handed coordinate system (projectile helicity frame). Similarly, the L' axis is oriented along the momentum of scattered protons, the N' axis is the same as the N axis, and the S' axis forms a right-handed coordinate system (outgoing particle helicity frame). The symbols A_N and P are analyzing power and vector polarization, respectively. The off-diagonal elements of PT observables $D_{I'J}$ between the horizontal and vertical axes vanish due to parity conservation.

The proton spin precesses around the vertical axis of the spectrometer. The spin precession angle χ with respect to the momentum direction of the proton is described by $\chi = \gamma(g/2-1)\alpha$ in the moving frame, where γ is a Lorentz factor defined by $\gamma=(m_pc^2+E_p)/m_pc^2$, g is the spin g factor of the proton, which is related to the proton magnetic moment by $\mu_p=\frac{1}{2}g\mu_N$ (μ_N is the nuclear magneton), and α is the bending angle of the spectrometer. The vertical ($p'_{N''}$) and horizontal ($p'_{S''}$) components of the polarization measured by the FPP are given as follows:

$$p'_{N''}=p'_{N'}=\frac{1}{1+p_N A_N}(P+D_{N'N}p_N), \quad (3a)$$

$$\begin{aligned} p'_{S''} &= p'_{S'}\cos\chi + p'_{L'}\sin\chi \\ &= \frac{1}{1+p_N A_N}[(D_{S'S}p_S + D_{S'L}p_L)\cos\chi \\ &\quad + (D_{L'S}p_S + D_{L'L}p_L)]\sin\chi. \end{aligned} \quad (3b)$$

In the measurement at 0°, the projectile helicity frame and the outgoing particle helicity frame are identical. In this case, off-diagonal components of the PT observables, analyzing power, and vector polarization vanish ($D_{SL}=D_{LS}=A_N=P=0$) due to the spatial rotational symmetry, and Eq. (3) reduces to

$$p'_{N''}=D_{N'N}p_N=D_{NN}p_N, \quad (4a)$$

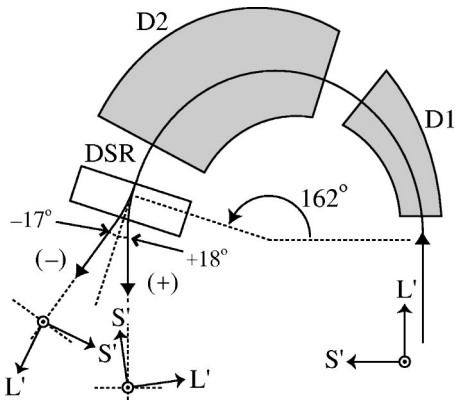

FIG. 2. Schematic description of the spin precession of horizontally polarized protons in the spectrometer Grand Raiden. Quadrupole and sextupole magnets of Grand Raiden are not shown for simplicity. For details see text.

$$\begin{aligned} p'_{S''} &= D_{S'S}p_S\cos\chi + D_{L'L}p_L\sin\chi \\ &= D_{SS}p_S\cos\chi + D_{LL}p_L\sin\chi. \end{aligned} \quad (4b)$$

The PT observables with nonprimed suffixes (D_{IJ}) in Eq. (4) are defined in the projectile helicity frame. The D_{IJ}'s are related to PT observables with primed suffixes ($D_{I'J}$) defined in the projectile helicity frame and the outgoing particle helicity frame by a spatial rotation of the coordinate system of outgoing particles. The D_{IJ}'s naturally become identical with the $D_{I'J}$'s at 0°.

Although the transverse diagonal components of PT observables have a simple relation $D_{SS}=D_{NN}$ at 0°, the D_{SS} and D_{NN} are treated as independent observables in this experiment. The reason is that the acceptance of the spectrometer Grand Raiden is not symmetrical with respect to vertical and horizontal directions ($|\theta_x|\leqslant 20$ mrad, $|\theta_y|\leqslant 35$ mrad) and this difference breaks the relation $D_{SS}=D_{NN}$ by $\approx 10\%$ at most.

The measurements were repeated using vertically polarized ($p_S=p_L=0$) and horizontally polarized ($p_N=0$) beams independently. In the measurements with a vertically polarized beam, the analyzing power was deduced from the asymmetry of the cross section by reversing the beam polarization. The vector polarization P and $D_{N'N}$ were deduced from simultaneous equations about $p'_{N''}$, which were obtained from Eq. (3a) for each polarizing direction in the reversing process.

Following Eqs. (3b) and (4b), two and four independent measurements of $p'_{S''}$ with horizontally polarized beams are generally required to obtain all horizontal PT observables at 0° and at other finite angles, respectively. On the basis of the mathematical considerations mentioned above, we measured $p'_{S''}$ under the two independent conditions with beam polarizations perpendicular to each other in the horizontal plane. In addition, for the measurements at finite angles, we used a special dipole magnet for spin rotation (DSR) [38] to increase the number of independent measurements. The DSR is a magnet that bends protons by $+18°$ or $-17°$ just in front of the focal plane of the spectrometer Grand Raiden as

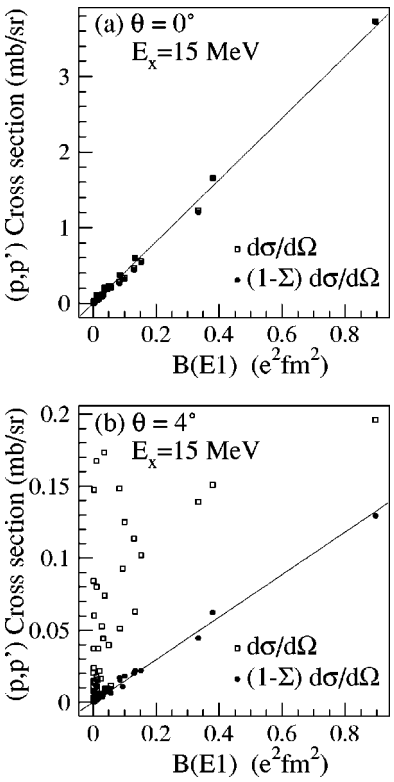

FIG. 3. Two-dimensional scatter plots of cross sections $[d\sigma/d\Omega,\ (1-\Sigma)d\sigma/d\Omega]$ at 0° (a) and 4° (b) calculated for 1^- shell model states. The open squares and solid circles indicate cross sections $(d\sigma/d\Omega)$ and non-spin-flip cross sections $[(1-\Sigma)d\sigma/d\Omega]$, respectively. The solid lines (shown to guide the eye) indicate proportional relations between $B(E1)$ and $(1-\Sigma)d\sigma/d\Omega$.

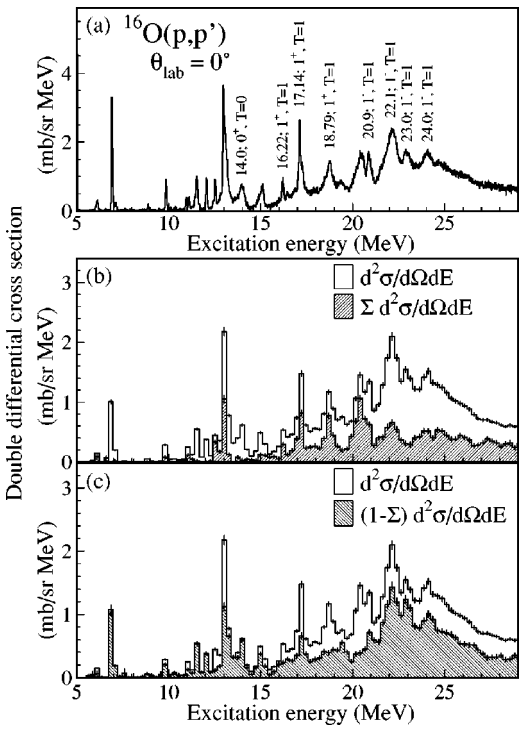

FIG. 4. Double differential cross sections for the $^{16}O(p,p')$ reaction at $E_p=392$ MeV and 0°. (a) $^{16}O(p,p')$ spectrum $d^2\sigma/d\Omega dE$. (b) Spin-flip component $\Sigma d^2\sigma/d\Omega dE$ is compared with $d^2\sigma/d\Omega dE$. (c) Non-spin-flip component $(1-\Sigma)d^2\sigma/d\Omega dE$ is compared with $d^2\sigma/d\Omega dE$.

shown in Fig. 2. The bending angles of scattered protons of the central ray are 180° and 145° for positive and negative polarities of the DSR, respectively. Then, the spin precession angles of 392-MeV protons in Grand Raiden are $\chi^{(+)}=458°$ and $\chi^{(-)}=369°$. The four independent measurements at finite angles were achieved by measuring the $p'_{S''}$ with both beam polarization axes for each DSR polarity. In the 0° measurement, the DSR was also used as a steering magnet with a bending angle of 1°–2° in order to correctly guide the proton beam into the beam dump. In this case, the spin precession angle in the spectrometer is $\chi\approx412°$ determined by the normal bending angle of 162° of Grand Raiden.

The reliability of our measurements was checked by measuring PT observables of proton-proton elastic scattering. We simultaneously measured protons scattered from hydrogen and oxygen in the ice target at $\theta_{lab}=6°-12°$ since the protons are still within the momentum acceptance of Grand Raiden. The measured PT observables for proton-proton elastic scattering agreed well with the result of the SAID calculation.

III. THEORETICAL CONSIDERATION

Microscopic distorted-wave impulse-approximation (DWIA) calculations for (p,p') reactions were performed using the computer codes DWBA98 and DWBB98 [39]. The effective nucleon-nucleon interaction derived by Franey and Love (FL) [40] at 425 MeV was used in the calculations. The global Dirac optical-model potential was used in the Schrödinger equivalent form [41]. This potential gives a good description for existing experimental data of elastic scattering on ^{16}O at 400 MeV [42]. The one-body transition density from the shell model calculation [23] was used in the present work. This shell model calculation was performed within the $(0+2)\hbar\omega$ and $(1+3)\hbar\omega$ configuration spaces for positive and negative parity states, respectively, with an interaction based on the Warburton-Brown potential [43] and CD Bonn potential [44]. The single-particle radial wave functions were obtained for a harmonic-oscillator potential with a size parameter of $\alpha=0.588$ fm^{-1}. The calculated observables were averaged over the acceptance of Grand Raiden ($|\theta_x|\leqslant20$ mrad, $|\theta_y|\leqslant35$ mrad) weighted by the calculated cross sections for comparison with the experimental data.

The spin-flip cross section $[d\sigma/d\Omega(\Delta S=1)]$ and non-spin-flip cross section $[d\sigma/d\Omega(\Delta S=0)]$ can be defined by

$$\frac{d\sigma}{d\Omega}(\Delta S=1)=\frac{3-(D_{SS}+D_{NN}+D_{LL})}{4}\left(\frac{d\sigma}{d\Omega}\right)\equiv\Sigma\left(\frac{d\sigma}{d\Omega}\right), \tag{5a}$$

$$\frac{d\sigma}{d\Omega}(\Delta S=0)=\frac{1+(D_{SS}+D_{NN}+D_{LL})}{4}\left(\frac{d\sigma}{d\Omega}\right)$$

$$\equiv(1-\Sigma)\left(\frac{d\sigma}{d\Omega}\right), \tag{5b}$$

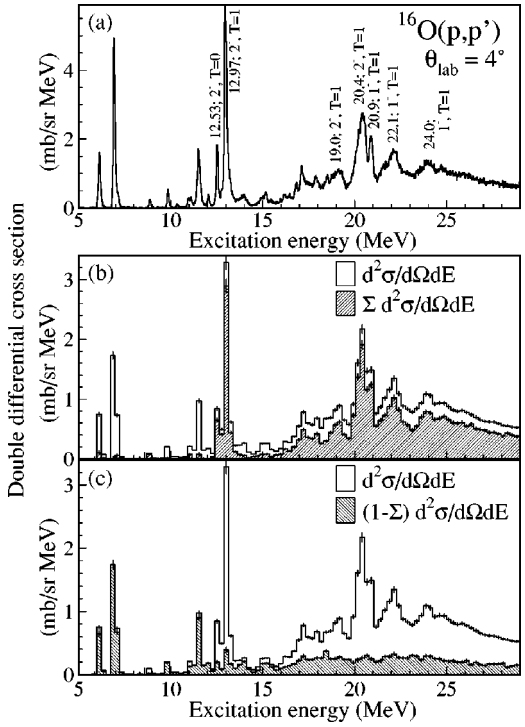

FIG. 5. Same as Fig. 4, but at a laboratory angle of 4°. The bumps at $E_x = 19.0$, 20.4, 20.9, 22.1, and 24.0 MeV are identified to be due to $\Delta L = 1$ transitions. Note that the bump at 23.0 MeV seen in Fig. 4 is missing.

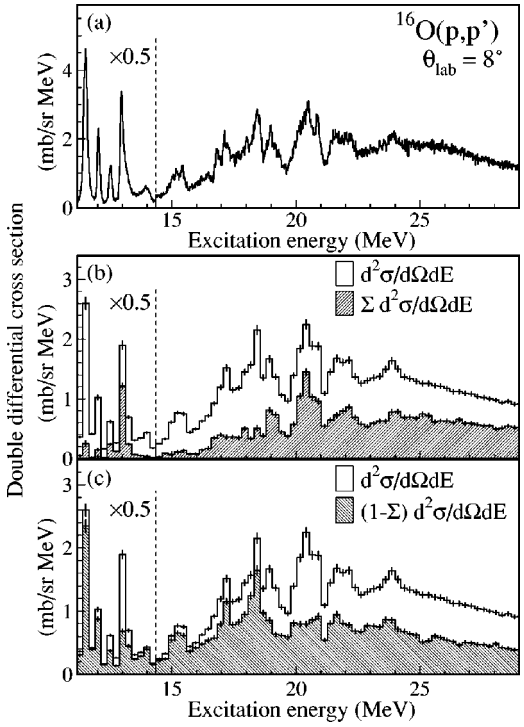

FIG. 6. Same as Fig. 4, but at a laboratory angle of 8°. The spectra below $E_x = 14.4$ MeV are scaled down by a factor of 0.5.

where $d\sigma/d\Omega$ is a differential cross section. PT observables in Eq. (5) are defined in the projectile helicity frame. It is known that the Σ value in Eq. (5) is unity for spin-flip transitions and zero for non-spin-flip transitions at forward scattering angles where the spin-orbit interaction is negligible [24,26]. This rule is well established for unnatural isovector transitions. For natural parity transitions, it is valid within 5% accuracy for $\theta \leqslant 5°$.

To verify the applicability of this rule, $d\sigma/d\Omega$ and $(1-\Sigma)d\sigma/d\Omega$ were calculated by DWIA for isovector 1^- states generated in the shell model space and were compared with the calculated $B(E1)$ values, which are good measures for non-spin-flip transition strengths. The IVGDR is strongly excited by the Coulomb interaction at 0°. The $d\sigma/d\Omega$ in Coulomb excitation decreases with increasing excitation energy since the virtual photon flux during the collision becomes rapidly small as a function of energy. Therefore, all the calculations were performed at an excitation energy of $E_x = 15$ MeV in order to fix the kinematic conditions.

The results are shown in the scatter plots of Fig. 3. The non-spin-flip strengths are dominant compared to the spin-flip strengths at 0° due to the Coulomb excitation of the IVGDR. Therefore, the strong linear correlation in the scatter plots at $\theta = 0°$ [shown in Fig. 3(a)] is interpreted as an indication that the cross sections observed at 0° are nearly proportional to the $E1$ transition strengths. The non-spin-flip cross sections are quenched at backward angles due to the destructive interference effect between the Coulomb (V_c) and isovector (V_τ) interactions. Non-spin-flip cross sections have values much smaller than the cross sections at $\theta = 4°$ as shown in Fig. 3(b). However, the correlation between non-spin-flip cross sections and $B(E1)$'s is still linear. Thus, we conclude that the transition strengths are reasonably separated into the spin-flip and non-spin-flip components by using Σ even at 4°.

IV. RESULTS AND DISCUSSION

The double differential cross sections at $\theta_{lab} = 0°$, 4°, and 8° for the ^{16}O(p,p') reaction at $E_p = 392$ MeV are shown in Figs. 4, 5, and 6, respectively. At 8°, the ^{16}O(p,p') spectra are obscured in the energy region of $E_x = 6-11$ MeV due to the large background originating from hydrogen in the ice target. Therefore, the spectra in Fig. 6 are only shown for the energy region of $E_x = 11.2-29$ MeV.

All low-lying discrete peaks observed between 6.05 MeV and 13.09 MeV have been identified as those of known transitions [45]. Table I lists the 0° cross sections in the center of mass system for these known discrete states. In the measurement where the central ray is set at 0°, the average angle of acceptance of the spectrometer is 1.2°. The cross sections were obtained by fitting the ^{16}O(p,p') spectrum at 0°. In the fitting procedure, Lorentzian functions with central energies and widths taken from Ref. [45] were used. The Lorentzian functions were folded by using a peak shape taken from the narrow states at $E_x = 6.92$ and 7.12 MeV. Although broad resonance states at $E_x = 9.59$, 11.26, and 11.60 MeV were taken into account to improve the fit, cross sections of the transitions to these states are not shown in Table I because of the large uncertainties in the fit. Since the peaks of the broad states are relatively small, the inclusion of the broad states into the fit gives no significant influence in estimating

TABLE I. Discrete levels observed in the $^{16}O(p,p')$ reaction at $E_p=392$ MeV. Excitation energies (E_x), spin parities (J^π), isospins (T), widths (Γ), and level half-lives ($\tau_{1/2}$) are taken from Ref. [45]. Cross sections in the center of mass system were obtained by fitting the $^{16}O(p,p')$ spectrum at 0° (see text).

E_x (MeV)	J^π; T	Γ or $\tau_{1/2}$	$d\sigma/d\Omega(0°)_{\text{c.m.}}$ (μ b/sr)
6.05	0^+; 0	$\tau_{1/2}=67\pm5$ ps	10 ± 1
6.13	3^-; 0	$\tau_{1/2}=18.4\pm0.5$ ps	23 ± 1
6.92	2^+; 0	$\tau_{1/2}=4.7\pm0.13$ fs	249 ± 7
7.12	1^-; 0	$\tau_{1/2}=8.3\pm0.5$ fs	19 ± 1
8.87	2^-; 0	$\tau_{1/2}=125\pm11$ fs	12 ± 1
9.59	1^-; 0	$\Gamma=420\pm20$ keV	
9.85	2^+; 0	$\Gamma=0.62\pm0.1$ keV	64 ± 2
10.36	4^+; 0	$\Gamma=26\pm3$ keV	11 ± 1
10.96	0^-; 0	$\tau_{1/2}=5.5\pm3.5$ fs	22 ± 2
11.08	3^+; 0	$\Gamma<12$ keV	24 ± 2
11.10	4^+; 0	$\Gamma=0.28\pm0.05$ keV	
11.26	0^+; 0	$\Gamma=2.5$ MeV	
11.52	2^+; 0	$\Gamma=71\pm3$ keV	137 ± 5
11.60	3^-; 0	$\Gamma=800\pm100$ keV	
12.05	0^+; 0	$\Gamma=1.5\pm0.5$ keV	72 ± 3
12.44	1^-; 0	$\Gamma=91\pm6$ keV	36 ± 2
12.53	2^-; 0	$\Gamma=111\pm1$ eV	57 ± 2
12.80	0^-; 1	$\Gamma=40\pm4$ keV	24 ± 2
12.97	2^-; 1	$\Gamma=1.34\pm0.04$ keV	176 ± 6
13.02	2^+; 0	$\Gamma=150\pm10$ keV	498 ± 14
13.09	1^-; 1	$\Gamma=130\pm5$ keV	

the peak area of the extracted states. The 11.10-MeV state was not separated from the neighboring state at 11.08 MeV. Similarly, the 13.09 MeV state was not separated from the 13.02-MeV state. Therefore, the summed values of the cross sections for these neighboring states are shown in Table I.

It is known that low-lying states are mostly non-spin-flip states, called natural parity states. Therefore, these states are only observed in our non-spin-flip spectrum $[(1-\Sigma)d^2\sigma/d\Omega dE]$. Excitations of the isovector states in ^{16}O begin with $E_x=12.8$ MeV. The spin-flip states observed at 0° above the threshold energy ($E_x=12.8$ MeV) are expected to be mainly due to the isovector transitions, since the isovector spin term ($V_{\sigma\tau}$) in the effective interaction is much stronger than the isoscalar spin term (V_σ) at small momentum transfer. In fact, the spin-flip spectrum at 0° shown in Fig. 4(b) is quite similar to the high-resolution $^{16}O(p,n)$ spectra near 0° reported in Refs. [15,18] if the threshold energy for the isovector transitions is taken into account.

A state at $E_x\approx13$ MeV is strongly excited with both spin-flip and non-spin-flip components at 0°. The spin-flip component of this state significantly increases at 4° as shown in Fig. 5(b). We conclude that this state consists of the mixing of three discrete states; an isovector 1^- state at 13.09 MeV, which is strongly excited by the Coulomb interaction at 0°, an isoscalar 2^+ state at 13.02 MeV, and an isovector 2^- state at 12.97 MeV. Three 1^+ states at 16.22, 17.14, and 18.79 MeV observed in electron scattering [46] are also seen in the spin-flip spectra. The 14-MeV state, which has been tentatively assigned as 1^+ or 0^+ in Ref. [14], has no spin-flip strength at 0°. Thus, this state is inferred to be a 0^+ or 1^- natural parity state. Most probably, this state could correspond to the 0^+ state reported in the electron scattering experiment by Hyde-Wright [47].

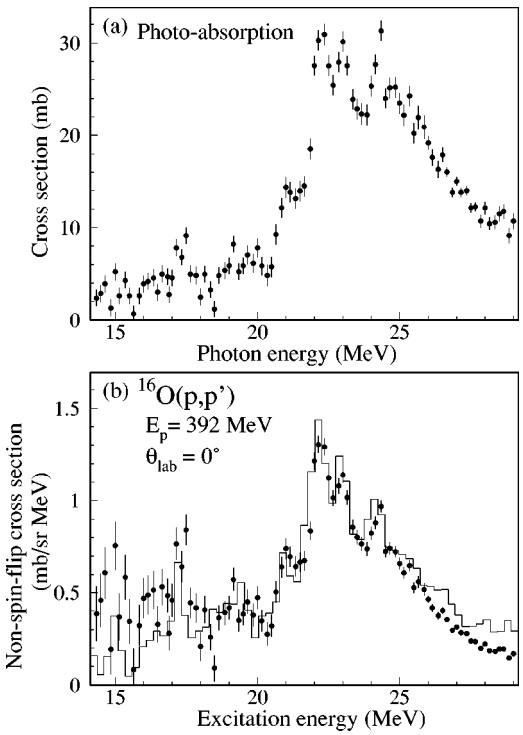

FIG. 7. (a) The photoabsorption spectrum from Ref. [48]. (b) Comparison of the non-spin-flip $^{16}O(p,p')$ spectrum at 0° (solid lines) and the corresponding converted photoabsorption spectrum (solid circles). See text for details. Measurement errors for the non-spin-flip spectrum are not shown in this figure for simplicity.

A. Non-spin-flip transitions

Four broad resonance states at 20.9, 22.1, 23.0, and 24.0 MeV are observed in the non-spin-flip spectrum at 0°. The cross sections of these non-spin-flip states are forward peaked, which could be characterized as IVGDR or $\Delta L=0$ transitions. The IVGDR in ^{16}O has been already well studied with electromagnetic probes. The total photoabsorption cross sections from Ref. [48] are shown in Fig. 7(a) as a function of photon energy. The relation between photoabsorption cross sections and the reduced $E1$ transition matrix element $B(E1)$ is given by Ref. [49],

$$\int \sigma_{abs}dE=\frac{16\pi^3}{9\hbar c}S(E1)$$
$$=\frac{16\pi^3}{9\hbar c}\sum_a (E_a-E_0)B(E1;0\rightarrow a), \qquad (6)$$

where $S(E1)$ is the first energy moment of the $B(E1)$ value. By using Eq. (6) and assuming the linear proportionality be-

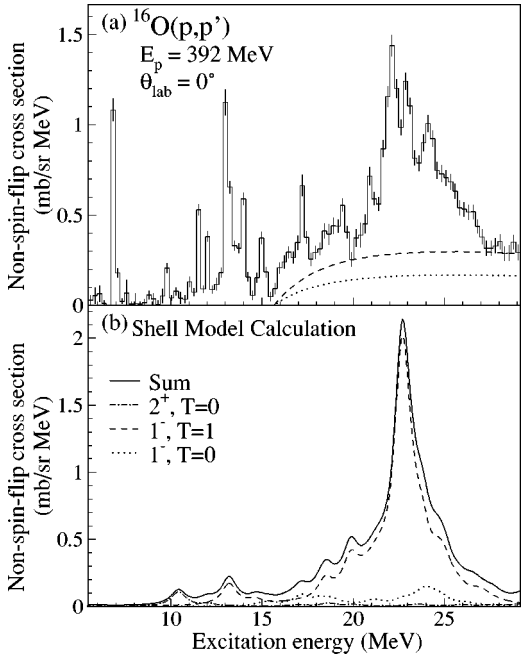

FIG. 8. (a) Measured non-spin-flip spectrum in the ^{16}O(p,p') reaction at 0°. The dashed and dotted lines show an empirical estimation of the quasifree continuum (see text). (b) Calculated non-spin-flip spectra obtained from the shell model calculation [23]. The solid line shows the sum of all the transitions up to $\Delta J=4$, although the contributions from $\Delta J=0$, 3, and 4 are small.

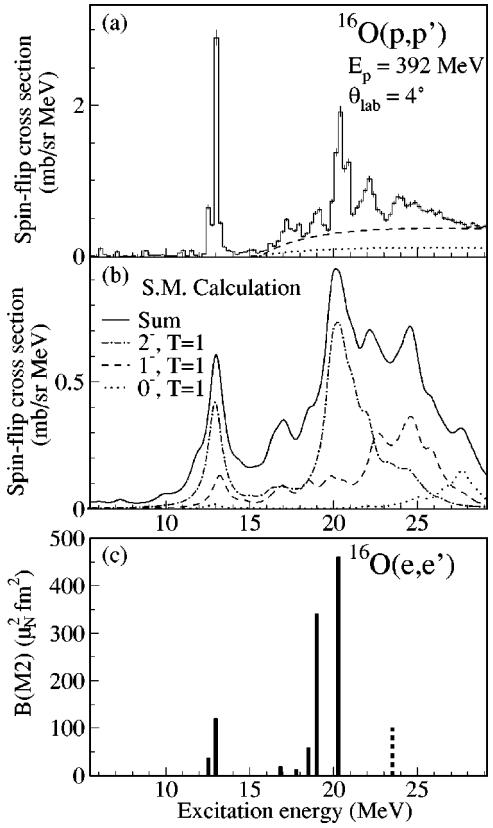

FIG. 9. (a) Measured spin-flip spectrum in the ^{16}O(p,p') reaction at $\theta_{lab}=4°$. The dashed and dotted lines show empirical estimations of the quasifree continuum (see text). (b) Calculated spin-flip spectra obtained from the shell model calculation [23]. The solid line shows the sum of all the transitions up to $\Delta J=4$. (c) Measured $M2$ strength distribution in ^{16}O from Ref. [46]. The state at $E_x=23.5$ MeV (dashed line) was tentatively assigned as 2^- in Refs. [52,54].

tween the $B(E1)$ value and non-spin-flip cross sections at 0°, our results can be directly compared to those from the photoabsorption experiment. The conversion factors from $B(E1)$ to non-spin-flip cross sections were deduced from DWIA calculations at each excitation energy to correct kinematic effects. Non-spin-flip 1^- transitions were assumed in the calculation. Their wave functions were obtained from a normal-mode procedure using the computer code NORMOD [50]. After multiplying the converted photon absorption spectrum by a factor of 1.3, the converted spectrum agrees well with the non-spin-flip spectrum from the (p,p') experiment as seen in Fig. 7(b). Contributions from the quasifree process and the monopole resonance have to be considered, since they might reduce the difference of the excitation strengths between the (p,p') results and the calculation that includes only the $E1$ transitions. The continuum due to the quasifree scattering and the isoscalar giant monopole resonance (ISGMR; $\Delta T=0$, $\Delta S=0$, $\Delta L=0$) are expected at the same energy region as the IVGDR in the (p,p') spectrum. However, the bumps due to the IVGDR are still observed in the residual spectrum after the calculated cross sections are subtracted from the non-spin-flip cross sections without any normalization factor. Thus, the normalization factor of 1.3 is required to explain the shape of the spectra. It is not clear why this normalization factor is needed.

We performed DWIA calculations using the shell model wave functions of Ref. [23] and the FL interaction of Ref. [40]. The calculated non-spin-flip cross sections were folded by assuming that each shell model state has a Lorentzian shape with a width of 1.0 MeV. In Fig. 8, the measured spectrum for the non-spin-flip cross sections at 0° is compared with those estimated from the DWIA calculation. The gross structure of the calculated spectrum was found to be similar to the observed one. The excitation energies of the discrete isovector 1^- state at $E_x=13.09$ MeV and the IVGDR located in the region of $E_x=20.9-24$ MeV are well explained. The IVGDR exhausts most of the non-spin-flip transition strengths in the calculation, while contributions from $\Delta L=0$ transitions discussed above are small. Recently, Lui *et al.* identified significant isoscalar $E0$ strengths exhausting (48 ± 10)% of the energy-weighted sum rule (EWSR) in the region of $E_x=11-40$ MeV by using the ^{16}O(α,α') reaction [51]. The shell model calculation [23] predicts isoscalar 0^+ strengths with 39.6% of the EWSR in the same energy region. Nevertheless, the summed (p,p') cross section for the 0^+ states is less than 7% of that for the IVGDR at 0° in our calculation. One of the reasons why the isoscalar 0^+ excitations are weak is that the isoscalar spin independent term V_0 in the effective interaction becomes small around $E_p=400$ MeV.

The summed value of the calculated non-spin-flip cross sections up to $E_x=29$ MeV is 7.57 mb/sr in the laboratory frame, while the experimental value is 9.47 ± 0.04 mb/sr. It

TABLE II. Comparison of the measured cross sections $(d\sigma/d\Omega)_{\text{c.m.}}$ and spin-flip cross sections $(\Sigma d\sigma/d\Omega)_{\text{c.m.}}$ with those from the DWIA calculation based on the shell model wave functions [23] for discrete $\Delta L=1$ transitions observed in the $^{16}O(p,p')$ reaction at $\theta_{\text{c.m.}}=4.4°$. Shell model states weaker than 0.01 mb/sr are not shown. Spin-flip cross sections for $E_x=7.12$ MeV and 10.96 MeV are not shown because of large uncertainties of the PT observables.

Experiment				Theory			
E_x (MeV)	$J^\pi; T$	$\frac{d\sigma}{d\Omega}(4.4°)_{\text{c.m.}}$ (μb/sr)	$\Sigma\frac{d\sigma}{d\Omega}(4.4°)_{\text{c.m.}}$ (μb/sr)	E_x (MeV)	$J^\pi; T$	$\frac{d\sigma}{d\Omega}(4.4°)_{\text{c.m.}}$ (μb/sr)	$\Sigma\frac{d\sigma}{d\Omega}(4.4°)_{\text{c.m.}}$ (μb/sr)
7.12	$1^-; 0$	48±2		6.04	$1^-; 0$	41	18
8.87	$2^-; 0$	25±1	19±2	7.28	$2^-; 0$	38	27
10.96	$0^-; 0$	25±2		9.84	$0^-; 0$	32	32
12.44	$1^-; 0$	37±6	164±12	11.38	$1^-; 0$	10	5
12.53	$2^-; 0$	179±30		11.84	$2^-; 0$	189	131
12.80	$0^-; 1$	42±2	600±24	12.90	$0^-; 1$	26	26
12.97	$2^-; 1$	534±15		12.94	$2^-; 1$	545	544
				13.12	$2^-; 0$	39	25
13.02	$2^+; 0$	490±15	342±20				
13.09	$1^-; 1$			13.21	$1^-; 1$	174	167

should be noted that the experimental value includes a contribution from the quasifree process. If we tentatively assume that a smooth continuum due to the quasifree process begins with the neutron emission threshold and increases with excitation energy as shown by a dashed line in Fig. 8(a), the non-spin-flip cross section of the quasifree process is estimated to be 3.35 mb/sr and the rest of the non-spin-flip cross section due to the resonant processes is 6.12 mb/sr, which is smaller by 20% than the predicted value. In the case when the magnitude of the quasifree continuum is multiplied by a factor of 0.6 as shown by the dotted line in Fig. 8(a), the experimental cross section for the resonant process becomes very close to the theoretical one.

B. Spin-flip transitions

In the spin-flip spectra shown in Figs. 4(b) and 5(b), broad bumps with $\Delta L=1$ were observed at $E_x=$ 19.0, 20.4, 20.9, 22.1, and 24.0 MeV. Since the bumps at 19.0 and 20.4 MeV are not seen in the non-spin-flip spectra [see Figs. 4(c) and 5(c)], they are inferred to be excited by unnatural parity transitions, and correspond to the SDR (2^-) reported in electron scattering [46,52,53]. The other resonances at 20.9, 22.1, and 24.0 MeV, which are seen in both the spin-flip and non-spin-flip spectra, could be due to 1^- excitations with a mixture of spin-flip and non-spin-flip characters. The resonance at 20.9 MeV was assigned as 2^- in Ref. [14], but our result favors the conclusion reported by Ref. [53] that the 20.9-MeV state is 1^-. A bump due to the excitation of a 1^- resonance at $E_x=23.0$ MeV is clearly seen in Fig. 4(c). However, the corresponding bump is not observed in the spin-flip spectrum at 4° [see Fig. 5(b)]. Thus, we conclude that the 1^- transition to the 23.0-MeV resonance is dominated by a non-spin-flip component.

In Figs. 9(a) and 9(c), the spin-flip spectrum at $\theta_{lab}=4°$ is compared with the results of electron scattering experiments of Ref. [46]. The spin parity of the state at $E_x=23.5$ MeV was tentatively assigned as $J^\pi=2^-$ in Refs. [52,54]. Our assignment for the SDR (2^-) is consistent with the result from the electron scattering experiments, but it is rather difficult to get a clear one-to-one correspondence for the 2^- states at 16.82, 17.78, 18.50, and 23.5 MeV in the present experiment. The ratio of the strength of the 20.4-MeV and 19.0-MeV resonance is quite different from the result obtained in electron scattering. This difference might be due to the contribution of the orbital part in the electromagnetic interaction, which does not give a sizable effect in (p,p') scattering at small momentum transfer.

The spin-flip spectrum from the DWIA calculation described above is presented in Fig. 9(b). Similarly to the non-spin-flip case, it is assumed that each shell model state has a Lorentzian shape with a width of 1.0 MeV. The calculation predicts a concentration of discrete spin-flip strengths at $E_x\approx13$ MeV, which is consistent with the experimental result. The theoretical and the experimental cross sections at $\theta_{\text{c.m.}}=4.4°$ (corresponding to $\theta_{lab}=4°$) for the discrete $\Delta L=1$ transitions are summarized in Table II. The two bumps observed at $E_x\approx13$ MeV [see Fig. 9(a)] are mainly due to the three $\Delta L=1$ states, i.e., the isoscalar 2^- state at 12.53 MeV, the isovector 2^- at 12.97 MeV, and the isovector 1^- at 13.09 MeV. The spin-flip cross sections for several weak states are not deduced separately since the PT observables for these states could not be extracted reliably. Their contributions are included in the values for the neighboring strong states. The theoretical calculation explains the cross sections $(d\sigma/d\Omega)$ and the spin-flip cross sections $(\Sigma d\sigma/d\Omega)$ for the discrete $\Delta L=1$ states quite well with the exception of the underestimated strengths of the isovector 1^- state at 13.09 MeV and the isoscalar 1^- state at 12.44 MeV.

In the region of giant resonances, the calculation reproduces the experimental result that the 2^- strength concentrates at an excitation energy below the 1^- strength. This ΔJ splitting is expected due to the spin-orbit interaction, supporting the validity of the present calculations. The strong resonance at 20.4 MeV is predominantly due to a 2^- transi-

tion, while the 22.1 MeV is due to both 2^- and 1^- transitions according to the calculation. In addition, the shell model calculation predicts a considerable 0^- strength at higher excitation energies. However, such a 0^- strength could not be separated reliably from the quasifree background. It is noteworthy to mention that a simple $1p$-$1h$ shell model calculation by Picklesimer and Walker [55] has predicted the gross structure of the SDR similar to the recent sophisticated calculation [23], although the quenching problem for spin excitations was not seriously discussed before the 1980s.

The sum of the experimental spin-flip cross sections up to $E_x=29$ MeV, which includes the continuum, is 9.10 ± 0.03 mb/sr in the laboratory frame, while that of the calculation is 7.99 mb/sr. Assuming a smooth quasifree continuum as shown in Fig. 9(a) by the dashed line, the spin-flip cross section due to the resonant processes is 5.06 mb/sr. This is smaller than the 7.99 mb/sr value from the calculation. The best agreement between experimental and calculated values is obtained if the estimated quasifree continuum is multiplied by a factor of 0.3 shown as a dotted line in Fig. 9(a).

V. SUMMARY AND CONCLUSION

In the present $^{16}O(p,p')$ experiment, spin-flip and non-spin-flip transitions were separated by measuring the polarization transfer (PT) observables. Strong peaks due to $M1$ transitions were observed at $E_x=16.22$, 17.14, and 18.77 MeV. The 14.0-MeV state, which was previously suggested to be excited by an $M1$ transition, is found to have a non-spin-flip nature.

Non-spin-flip transitions with forward peaked cross sections were observed at excitation energies between 20 MeV and 27 MeV. These transitions are well reproduced by a calculation in which the excitation strengths are converted from the photoabsorption cross sections with a normalization factor of 1.3. Therefore, we conclude that the major part of the IVGDR strength is exhausted in the resonance region of $E_x=20-27$ MeV. The recent shell model calculation [23] also supports this conclusion. One may address a question that a significant strength due to the 0^+ excitation could, in principle, exist in the IVGDR region. However, the contributions from the ISGMR are rather small according to the calculation.

Spin-flip strengths observed in the same energy region with the IVGDR are found to be excited with $\Delta L=1$ angular momentum transfer. The resonances observed at $E_x=20.9$, 22.1, and 24.0 MeV carry both IVGDR and SDR (1^-) strengths. The resonances at $E_x=19.0$ and 20.4 MeV are observed only in the spin-flip spectra and are, therefore, assigned to be 2^- states. The energies of strong 2^- states observed in the present (p,p') experiment agree well with those of the 2^- states at $E_x=12.53$, 12.97, 19.0, and 20.3 MeV reported in electron scattering studies [46,52–54]. However, the strength ratios of the 19.0- and 20.4-MeV states are different. This may be attributed to the intrinsic contribution of the orbital part in electron scattering. We observed that the major part of the SDR (2^-) strength in ^{16}O is located at excitation energies below the SDR (1^-) as seen in the $A=12$ system [8,10,13]. This result is consistent with the expectation that the three spin components of the SDR split in excitation energy in the order of $E_x(2^-)<E_x(1^-)<E_x(0^-)$. The shell model calculation [23] reproduces well the distribution of the 2^- and 1^- spin-flip strengths in ^{16}O measured in this study. This calculation predicts the existence of the 0^- transition at high excitation energies of about 27 MeV. However, not enough evidence to identify the 0^- strength could be found in the experiment because of its relatively weak excitation and the surrounding quasifree background. The experimental result from the present (p,p') study will be useful in estimating the neutrino absorption cross sections by ^{16}O in the supernova neutrino observatories.

ACKNOWLEDGMENTS

The authors would like to thank Professor J. Raynal, Professor K. Amos, Professor S. Karataglidis, and Professor S. Y. van der Werf for valuable discussions of theoretical calculations. We gratefully acknowledge the outstanding effort of the RCNP cyclotron staff for providing the clean stable beam. This research program was supported in part by the Research Fellowships of the Japan Society for the Promotion of Science (JSPS) for Young Scientists, the U.S.-Japan Cooperative Science Program of the JSPS, and NSF Grant No. PHY-007911.

[1] W. P. Alford and B. M. Spicer, Adv. Nucl. Phys. **24**, 1 (1998), and references therein.
[2] M. Fujiwara, H. Akimune, I. Daito, H. Ejiri, Y. Fujita, M. B. Greenfield, M. N. Harakeh, T. Inomata, J. Jänecke, S. Nakayama, N. Takemura, A. Tamii, M. Tanaka, H. Toyokawa, and M. Yosoi, Nucl. Phys. **A599**, 223c (1996).
[3] E. Kolbe and K. Langanke, Phys. Rev. C **63**, 025802 (2001).
[4] G. M. Fuller, W. C. Haxton, and G. C. McLaughlin, Phys. Rev. D **59**, 085005 (1999).
[5] K. Langanke, P. Vogel, and E. Kolbe, Phys. Rev. Lett. **76**, 2629 (1996).
[6] F. T. Baker, L. Bimbot, C. Djalali, C. Glashausser, H. Lenske, W. G. Love, M. Morlet, E. Tomasi-Gustafsson, J. Van de Wiele, J. Wambach, and A. Willis, Phys. Rep. **289**, 235 (1997).
[7] H. Sagawa and B. Castel, Nucl. Phys. **A435**, 1 (1985).
[8] C. Gaarde, J. S. Larsen, H. Sagawa, N. Ohtsuka, J. Rapaport, T. N. Taddeucci, C. D. Goodman, C. C. Foster, C. A. Goulding, D. Horen, T. Masterson, and E. Sugarbaker, Nucl. Phys. **A422**, 189 (1984).
[9] F. T. Baker, D. Beatty, L. Bimbot, V. Cupps, C. Djalali, R. W. Fergerson, C. Glashausser, G. Graw, A. Green, K. Jones, M. Morlet, S. K. Nanda, A. Sethi, B. H. Storm, W. Unkelbach, and A. Willis, Phys. Rev. C **48**, 1106 (1993).
[10] X. Yang, L. Wang, J. Rapaport, C. D. Goodman, C. Foster, Y. Wang, W. Unkelbach, E. Sugarbaker, D. Marchlenski, S. de Lucia, B. Luther, J. L. Ullmann, A. G. Ling, B. K. Park, D. S.

Sorenson, L. Rybarcyk, T. N. Taddeucci, C. R. Howell, and W. Tornow, Phys. Rev. C **48**, 1158 (1993).
[11] H. Okamura, S. Fujita, Y. Hara, K. Hatanaka, T. Ichihara, S. Ishida, K. Katoh, T. Niizeki, H. Ohnuma, H. Otsu, H. Sakai, N. Sakamoto, Y Satou, T. Uesaka, T. Wakasa, and T. Yamashita, Phys. Lett. B **345**, 1 (1995).
[12] Toshio Suzuki and H. Sagawa, Nucl. Phys. **A637**, 547 (1998).
[13] T. Inomata, H. Akimune, I. Daito, H. Ejiri, H. Fujimura, Y. Fujita, M. Fujiwara, M. N. Harakeh, K. Ishibashi, H. Kohri, N. Matsuoka, S. Nakayama, A. Tamii, M. Tanaka, H. Toyokawa, M. Yoshimura, and M. Yosoi, Phys. Rev. C **57**, 3153 (1998).
[14] C. Djalali, G. M. Crawley, B. A. Brown, V. Rotberg, G. Caskey, A. Galonsky, N. Marty, M. Morlet, and A. Willis, Phys. Rev. C **35**, 1201 (1987).
[15] A. Fazely, B. D. Anderson, M. Ahmad, A. R. Baldwin, A. M. Kalenda, R. J. McCarthy, J. W. Watson, R. Madey, W. Bertozzi, T. N. Buti, J. M. Finn, M. A. Kovash, B. Pugh, and C. C. Foster, Phys. Rev. C **25**, 1760 (1982); **26**, 746(E) (1982).
[16] K. H. Hicks, A. Celler, O. Häusser, R. Henderson, K. P. Jackson, B. Pointon, J. Rapaport, M. Vetterli, and S. Yen, Phys. Rev. C **43**, 2554 (1991).
[17] D. J. Mercer, J. Rapaport, C. A. Whitten, Jr., D. Adams, R. Byrd, X. Y. Chen, A. Fazely, T. Gaussiran, E. Gülmez, C. Goodman, D. W. Huang, G. Igo, A. Ling, D. Marchlenski, D. Prout, L. Rybarcyk, E. Sugarbaker, and T. N. Taddeucci, Phys. Rev. C **49**, 3104 (1994).
[18] J. W. Watson, B. D. Anderson, A. R. Baldwin, C. C. Foster, D. Lamm, R. Madey, M. R. Plumley, and P. J. Pella, Nucl. Phys. **A577**, 79c (1994).
[19] E. Kolbe, K. Langanke, S. Krewald, and F.-K. Thielemann, Nucl. Phys. **A540**, 599 (1992).
[20] H. Ejiri, Phys. Rep. **338**, 265 (2000).
[21] Toshio Suzuki, in *Proceedings of the RCNP-TMU Symposium, Tokyo Metropolitan University, Japan*, edited by H. Yabu, T. Suzuki, and H. Toki (World Scientific, Singapore, 2000), p. 73.
[22] T. Siiskonen, Phys. Rev. C **54**, 045501 (2001).
[23] N. Auerbach and B. A. Brown, Phys. Rev. C **65**, 024322 (2002).
[24] A. Tamii, H. Akimune, I. Daito, Y. Fujita, M. Fujiwara, K. Hatanaka, K. Hosono, F. Ihara, T. Inomata, T. Ishikawa, M. Itoh, M. Kawabata, T. Kawabata, M. Nakamura, T. Noro, E. Obayashi, H. Sakaguchi, H. Takeda, T. Taki, H. Toyokawa, H. P. Yoshida, M. Yoshimura, and M. Yosoi, Phys. Lett. B **459**, 61 (1999).
[25] T. Ishikawa, H. Akimune, I. Daito, H. Fujimura, Y. Fujita, M. Fujiwara, K. Hatanaka, K. Hosono, F. Ihara, M. Itoh, T. Kawabata, M. Nakamura, T. Noro, E. Obayashi, H. Sakaguchi, A. Tamii, H. Takeda, T. Taki, H. Toyokawa, H. P. Yoshida, M. Yoshimura, and M. Yosoi, Nucl. Phys. **A687**, 58c (2001).
[26] H. Sakai, T. Wakasa, H. Okamura, T. Nonaka, T. Ohnishi, K. Yako, K. Sekiguchi, S. Fujita, Y. Satou, H. Otsu, T. Uesaka, S. Ishida, N. Sakamoto, M.B. Greenfield, and K. Hatanaka, in *Proceedings of the International Symposium of New Facet of Spin Giant Resonances in Nuclei, Tokyo, Japan, 1997*, edited by H. Sakai, H. Okamura, and T. Wakasa (World Scientific, Singapore, 1998), p. 29.
[27] T. Suzuki, Prog. Theor. Phys. **103**, 859 (2000).
[28] K. Hatanaka, K. Takahisa, H. Tamura, M. Sato, and I. Miura, Nucl. Instrum. Methods Phys. Res. A **384**, 575 (1997).
[29] M. Fujiwara, H. Akimune, I. Daito, H. Fujimura, Y. Fujita, K. Hatanaka, H. Ikegami, I. Katayama, K. Nagayama, N. Matsuoka, S. Morinobu, T. Noro, M. Yoshimura, H. Sakaguchi, Y. Sakemi, A. Tamii, and M. Yosoi, Nucl. Instrum. Methods Phys. Res. A **422**, 484 (1999).
[30] M. Yosoi, H. Akimune, I. Daito, H. Fujimura, Y. Fujita, M. Fujiwara, K. Hatanaka, K. Hosono, T. Inomata, T. Ishikawa, M. Itoh, M. Kawabata, T. Kawabata, M. Nakamura, T. Noro, E. Obayashi, H. Sakaguchi, H. Takeda, T. Taki, A. Tamii, H. Toyokawa, M. Uchida, H. P. Yoshida, and M. Yoshimura, in *Spin 2000*, edited by K. Hatanaka, T. Nakano, K. Imai, and H. Ejiri, AIP Conf. Proc. No. 570 (AIP, New York, 2001), p. 765.
[31] T. Kawabata, H. Akimune, H. Fujimura, H. Fujita, Y. Fujita, M. Fujiwara, K. Hara, K. Hatanaka, K. Hosono, T. Ishikawa, M. Itoh, J. Kamiya, M. Nakamura, T. Noro, E. Obayashi, H. Sakaguchi, Y. Shimbara, H. Takeda, T. Taki, A. Tamii, H. Toyokawa, N. Tsukahara, M. Uchida, H. Ueno, T. Wakasa, K. Yamasaki, Y. Yasuda, H. P. Yoshida, and M. Yosoi, Nucl. Instrum. Methods Phys. Res. A **459**, 171 (2001).
[32] N. Matsuoka, T. Noro, K. Tamura, M. Yoshimura, M. Yosoi, A. Okihana, and T. Yoshimura, Phys. Lett. B **359**, 39 (1995), and references therein.
[33] R. A. Arndt, C. H. Oh, I. I. Strakovsky, R. L. Workman, and F. Dohrmann, Phys. Rev. C **56**, 3005 (1997); solution SP00 from SAID website (http://gwdac.phys.gwu.edu).
[34] M. Yosoi, H. Akimune, I. Daito, M. Fujiwara, S. Hirata, T. Inomata, O. Kamigaito, M. Kawabata, T. Noro, Y. Sakemi, T. Takahashi, A. Tamii, S. Toyama, A. Yamagoshi, M. Yoshimura, and H. Sakaguchi, in *High Energy Spin Physics*, edited by K. J. Heller and S. L. Smith, AIP Conf. Proc. No. 343 (AIP, New York, 1995), p. 157.
[35] M. W. McNaughton, B. E. Bonner, H. Ohnuma, O. B. Van Dijk, Sun Tsu-Hsun, C. L. Hollas, D. J. Cremans, K. H. McNaughton, P. J. Riley, R. F. Rodebaugh, Shen-Wu Xu, S. E. Turpin, B. Aas, and G. S. Weston, Nucl. Instrum. Methods Phys. Res. A **241**, 435 (1985).
[36] N. Hoshizaki, J. Phys. Soc. Jpn. **55**, 549 (1986), and references therein.
[37] G. G. Ohlsen, Rep. Prog. Phys. **35**, 717 (1972).
[38] M. Fujiwara, S. Morinobu, M. Yosoi, and H. Ikegami, National Superconducting Cyclotron Laboratory, Technical Report No. MSUCL-685, 1989 (unpublished), p. 283.
[39] J. Raynal, program DWBA98 NEA 1209/05, 1999.
[40] M. A. Franey and W. G. Love, Phys. Rev. C **31**, 488 (1985).
[41] S. Hama, B. C. Clark, E. D. Cooper, H. S. Sherif, and R. L. Mercer, Phys. Rev. C **41**, 2737 (1990).
[42] C. Chan, M.S. thesis, University of Alberta, 1985; the data of the elastic proton scattering on ^{16}O at 400 MeV are cited by Ch. Elster, S. P. Weppner, and C. R. Chinn, Phys. Rev. C **56**, 2080 (1997).
[43] E. K. Warburton and B. A. Brown, Phys. Rev. C **46**, 923 (1992).
[44] R. Machleidt, F. Sammarruca, and Y. Song, Phys. Rev. C **53**, 1483 (1996).
[45] D. R. Tilley, H. R. Weller, and C. M. Cheves, Nucl. Phys. **A564**, 1 (1993).
[46] G. Küchler, A. Richter, E. Spamer, W. Steffen, and W. Knüpfer, Nucl. Phys. **A406**, 473 (1983).
[47] C. Hyde-Wright, Ph.D. thesis, MIT, 1984.

[48] J. Ahrens, H. Borchert, K. H. Czock, H. B. Eppler, H. Gimm, H. Gundrum, M. Kröning, P. Riehn, G. Sita Ram, A. Zieger, and B. Ziegler, Nucl. Phys. **A251**, 479 (1975).
[49] A. Bohr and B. R. Mottelson, *Nuclear Structure* (Benjamin, New York, 1975), Vol. 2, p. 478.
[50] S. Y. van der Werf, computer code NORMOD (unpublished).
[51] Y.-W. Lui, H. L. Clark, and D. H. Youngblood, Phys. Rev. C **64**, 064308 (2001).
[52] A. Goldmann and M. Stroetzel, Phys. Lett. **31B**, 287 (1970).
[53] M. Stroetzel and A. Goldmann, Z. Phys. **233**, 245 (1970).
[54] A. Goldmann and M. Stroetzel, Z. Phys. **239**, 235 (1970).
[55] A. Picklesimer and G. E. Walker, Phys. Rev. C **17**, 237 (1978).